

# Correlation of PET-MRI, Pathology, LOH, and Surgical Success in a Case of CHI With Atypical Large Pancreatic Focus

Hendrik Vosschulte,<sup>1</sup> Konrad Mohnike,<sup>2</sup> Klaus Mohnike,<sup>3</sup> Katharina Warncke,<sup>4</sup>  
Ayse Akcay,<sup>5</sup> Martin Zenker,<sup>6</sup> Ilse Wieland,<sup>6</sup> Ina Schanze,<sup>6</sup> Julia Hoefele,<sup>7</sup> Christine Förster,<sup>8</sup>  
Winfried Barthlen,<sup>1</sup> Kim Stahlberg,<sup>1</sup> and Susann Empting<sup>3</sup>

<sup>1</sup>Department of Pediatric Surgery, Protestant Hospital of Bethel Foundation, University Hospital OWL, Campus Bielefeld Bethel, University of Bielefeld, 33617 Bielefeld, Germany

<sup>2</sup>DTZ Diagnostic and Therapeutic Center, 10243 Berlin, Germany

<sup>3</sup>University Children's Hospital, Otto-von-Guericke University Magdeburg, 39120 Magdeburg, Germany

<sup>4</sup>Department of Pediatrics, Kinderklinik München Schwabing, Technical University of Munich, School of Medicine, 80804 Munich, Germany

<sup>5</sup>Department of Neonatology, Munich-Schwabing Municipal Hospitals, 80804 Munich, Germany

<sup>6</sup>Institute of Human Genetics, University Hospital, Otto-von-Guericke University Magdeburg, 39120 Magdeburg, Germany

<sup>7</sup>Institute of Human Genetics, Klinikum rechts der Isar, Technical University of Munich, School of Medicine, 81675 Munich, Germany

<sup>8</sup>Institute of Pathology, Hospital Nordstadt, affiliated with the University Hospital of the University of Bielefeld, Campus Bielefeld Bethel, Hanover, 33617 Bielefeld, Germany

**Correspondence:** Hendrik Vosschulte, MD, Department of Pediatric Surgery, Protestant Hospital of Bethel Foundation, University Hospital OWL, Campus Bielefeld Bethel, University of Bielefeld, Burgsteig 13, 33617 Bielefeld, Germany. Email: [hendrik.vosschulte@evkb.de](mailto:hendrik.vosschulte@evkb.de)

## Abstract

Congenital hyperinsulinism (CHI) is a rare cause of severe hypoglycemia in newborns. In focal CHI, usually one activity peak in fluorine-18-L-dihydroxyphenylalanine (<sup>18</sup>F-DOPA) positron emission tomography–magnetic resonance imaging (PET-MRI) indicates one focal lesion and its resection results in cure of the child. We present the case of a 5-month-old girl with CHI. Mutational screening of genes involved in CHI revealed a heterozygous pathogenic variant in the *ABCC8* gene, which was not detectable in the parents. <sup>18</sup>F-DOPA PET-MRI revealed 2 distinct activity peaks nearby in the pancreatic body and neck. Surgical resection of the tissue areas representing both activity peaks resulted in long-lasting normoglycemia that was proven by a fasting test. Molecular analysis of tissue samples from various sites provided evidence that a single second genetic hit in a pancreatic precursor cell was responsible for the atypical extended pancreatic lesion. There was a close correlation in the resected areas of PET-MRI activity with focal histopathology and frequency of the mutant allele (loss of heterozygosity) in the tissue. Focal lesions can be very heterogeneous. The resection of the most affected areas as indicated by imaging, histopathology, and genetics could result in complete cure.

**Key Words:** congenital hyperinsulinism, large focal lesion, hypoglycemia, focal chi, pediatric surgery, <sup>18</sup>F, Dopa

**Abbreviations:** 3D, 3 dimensional; <sup>18</sup>F-DOPA, fluorine-18-L-dihydroxyphenylalanine; ATP, adenosine triphosphate; BWS, Beckwith-Wiedemann syndrome; CHI, congenital hyperinsulinism; GRE, gradient-echo; K-ATP, adenosine 5'-triphosphate–sensitive potassium; LOH, loss of heterozygosity; MAF, mutant allele fraction; MRI, magnetic resonance imaging; PET, positron emission tomography; SMV, superior mesenteric vein; UPD, uniparental disomy.

Congenital hyperinsulinism (CHI) is a rare cause of sudden hypoglycemia in newborns with an incidence of 1:40 000 [1]. It can lead to life-threatening events and continuous neurological damage if not treated adequately [2, 3]. CHI is caused by (likely) pathogenic variants in components of the regulatory circuit in pancreatic  $\beta$  cells, which lead to uncontrolled production and secretion of insulin [4]. Most authors describe 3 forms of CHI: diffuse, focal, and atypical CHI [5]. Whereas in diffuse CHI all pancreatic islet cells are affected, in focal CHI there is usually only one small, defined area of pathological cells. The removal of this focal lesion results in surgical cure [6, 7]. In atypical CHI there is often a coexistence of enlarged and small suppressed islets with different insulin expression. The pathological

alterations may show a segmental distribution, and efficient surgical treatment is challenging [5].

Defects of the adenosine 5'-triphosphate–sensitive potassium (K-ATP) channels of pancreatic  $\beta$  cells, which are encoded by *ABCC8* and *KCNJ11*, represent the most common mechanism for CHI. While biallelic recessively inherited and heterozygous dominantly acting variants in these genes are associated with a diffuse type of CHI, the presence of a loss-of-function variant on the paternal allele together with a second genetic hit in the affected pancreatic tissue—mostly by uniparental disomy (UPD) 11p causing loss of the maternally inherited wild-type allele—represents the typical mechanism in focal CHI [4].

Recently, Tung et al [8] described an unusual phenotype with multiple foci of adenomatous hyperplasia throughout the pancreas in an infant with a paternal inherited pathogenic *ABCC8* mutation and UPD detected in pancreatic tissue but absent in peripheral leucocytes.

We describe an unusual case of a large, heterogeneous focal lesion in the pancreas of a 5-month-old girl with CHI. Two distinct activity peaks that were seen on positron emission tomography–magnetic resonance imaging (PET-MRI) correlated with histopathological changes and genetically proven loss of heterozygosity (LOH) caused by UPD 11p. As the surgical removal of these areas resulted in long-lasting normoglycemia without medication, these regions must have represented the main source of uncontrolled insulin secretion.

## Clinical Presentation

A 5-month-old girl suffered from hypoglycemia since birth. She was born in the 38 + 3 weeks of gestation (weight 3560 g, length 52 cm). On her first day of life, she presented with irritability and tremors with minimal blood glucose levels of 32 mg/dL (1.8 mmol/L). CHI was diagnosed on the basis of recurrent nonketotic hypoglycemia and inappropriately elevated insulin and c-peptide levels in a hypoglycemic state (insulin 14.6  $\mu$ IU/mL, c-peptide 3.55 ng/mL). There were 2 other measurements during hypoglycemic episodes confirming hyperinsulinemia (insulin 13.5  $\mu$ IU/mL and 11.0  $\mu$ IU/mL, c-peptide 2.4 ng/mL and 2.6 ng/mL, respectively). Subcutaneous glucagon injection during hypoglycemia resulted in a substantial increase of blood glucose levels from 41 mg/dL to 66 mg/dL after administration.

Diazoxide (15 mg/kg/d) given for 27 days had no considerable effect on the hypoglycemic conditions. Starting octreotide (4  $\times$  50  $\mu$ g subcutaneously per day) combined with 1 g maltodextrin per 100 mL nourishment ensured stabilization of blood glucose levels. At presentation in our reference center for CHI, she required 65  $\mu$ g octreotide 3 times a day and 110 mL milk with 10 g maltodextrin added every 3 hours to obtain a blood glucose level between 90 and 120 mg/dL.

## Genetic Diagnostics in the Family

Genetic examination of a peripheral blood DNA sample from the girl was performed by standard exome-based analysis of CHI genes. Only one heterozygous variant in the *ABCC8* gene was identified. The detected c.2521C > T variant in *ABCC8* generates a premature stop codon (p.Arg841Ter) and is predicted to cause a truncation of the encoded protein or absence of the protein due to nonsense-mediated decay. This variant has been repeatedly observed as a loss-of-function allele in autosomal recessive and focal *ABCC8*-related CHI and is classified as pathogenic by ClinVar (ClinVar accession No.: VCV000996301.1). Targeted genetic examination of the parents showed that neither of them carried the *ABCC8* variant, thus indicating a de novo occurrence in the child. Assuming that the de novo event arose on the paternal allele, this genetic constellation was considered compatible with a focal type of CHI. Methylation-specific multiplex ligation-dependent probe amplification (MS-MLPA) analysis at the Beckwith-Wiedemann syndrome (BWS) region on chromosome 11p15 showed a normal pattern in leukocyte DNA from the child (data not shown).

## Positron Emission Tomography–Magnetic Resonance Imaging

We generally use PET-MRI (3Tesla mMR, Siemens) to examine patients suspected of focal CHI to avoid exposure to radiation, which is substantial in a PET-computed tomography scan and because of improved soft-tissue contrast of the MRI part, sometimes even allowing us to distinguish the pancreatic duct. The upper ventral scan was commenced directly after injection of 34 MBq fluorine-18-L-dihydroxyphenylalanine ( $^{18}$ F-DOPA); thereafter, scans were performed up to 60 minutes post injection. The examination was conducted with the patient under analgosedation.

MRT upper ventral region was performed with the following parameters: transversal gradient echo (GRE) with transversal diffusion weighting; MR cholangiopancreatography with 3-dimensional (3D) reconstruction by the maximum intensity projection method after intravenous administration of contrast agent (4 mL Dotarem) with GRE 3D T1-weighted VIBE transversal; slice thickness between 1.5 mm and 2 mm; postcontrast GRE 3D T1-weighted VIBE transversal/coronal.

In the PET-MRI with  $^{18}$ F-DOPA in the fifth month of life, a complex finding appeared that differentially corresponded to an unaffected pancreatic tail about 3 cm in length and then 2 distinct activity peak areas that appeared suspicious for focal lesions in the pancreatic neck and pancreatic corpus, 1 to the right (Fig. 1A) and 1 to the left (Fig. 1B) of the superior mesenteric vein.

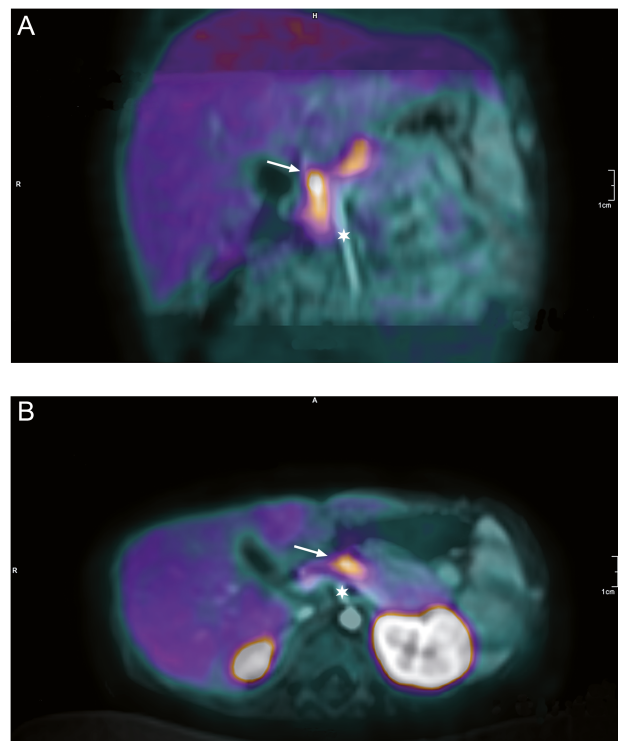


**Figure 1.** A, Positron emission tomography–magnetic resonance imaging (PET-MRI) fused coronal view with MR sequence: possible focal area (arrow) in the pancreatic head near to the body (immediately right and right ventral to the superior mesenteric vein [star]). B, PET-MRI fused axial view with MR sequence: possible focal area in the pancreatic corpus (arrow) near the tail (3 mm left ventral to the steeply descending superior mesenteric vein [star]).

## Surgery

Laparotomy was performed under general anesthesia. Fig. 2 shows the macroscopic appearance of the pancreas before resection, which was macroscopically normal. Biopsies of 1 to 3 mm in diameter were taken from the pancreas and sent for frozen section. Two areas on the ventral side, right and left of the mesenteric vein according to the PET-MRI hyperactivity areas, were found to show focal morphology in frozen section according to the definition by Rahier and colleagues [9]. The tissue between them was ambiguous in histopathology and termed *abnormal architecture*. All other biopsies showed normal or suppressed pancreatic islet cells. Both of the 2 suspicious areas were resected, taking care not to touch the pancreatic duct. There was no capsule. The area in between was left in place (Fig. 3).

The postoperative course was uneventful. Instantly after surgery, the blood glucose levels maintained stable at a level between 60 and 110 mg/dL without medication or starch enrichment. The drain was removed after 6 days and normal nutrition steadily increased. Discharge from the hospital took place day 13.

At follow-up 3 months after the procedure, the girl showed normal 24-hour blood glucose values without medication or

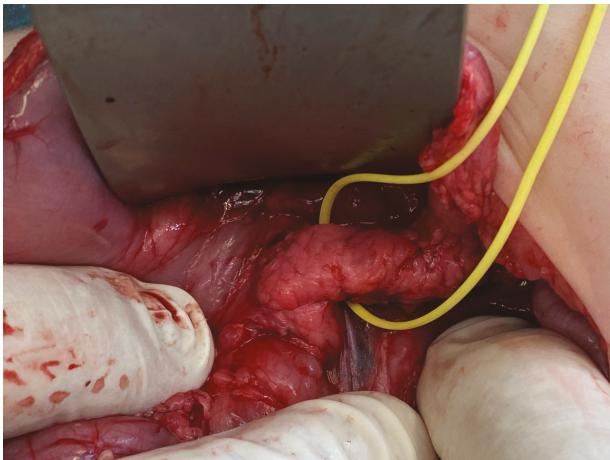


**Figure 2.** Pancreas before taking biopsies. The yellow loop is above the superior mesenteric vein.



**Figure 3.** Appearance of the pancreas after resection of the focal areas right and left to the superior mesenteric vein.

food supplement. A 12-hour fast showed normal results with blood glucose levels greater than 70 mg/dL (3.9 mmol/L) interpreted as normoglycemia. Cognitive, speech, and motor development were assessed using the Bailey scales of infant and toddler development (third edition) and showed age-appropriate development.

## Histopathology

Immunohistochemical stainings were performed by using the automated immunohistochemistry and in situ hybridization platform Dako Omnis (DAKO, Agilent) according to the manufacturer's instructions. Used antibodies were anti-chromogranin A, anti-synaptophysin, anti-inhibin (Table 1). Visualization was performed on an EnVision FLEX, High pH system (DAKO, Agilent) according to the manufacturer's guidelines.

## Staining Details

The system detects primary mouse and rabbit antibodies and the reaction is visualized by EnVision FLEX DAB + Chromogen. Before staining, formalin-fixed, paraffin-embedded tissue sections are subjected to onboard deparaffinization and hydration followed by heat-induced epitope retrieval using the target retrieval reagent specified in the package insert for the primary antibody. The kit includes EnVision FLEX Target Retrieval Solution, High pH. Endogenous peroxidase should be blocked with EnVision FLEX Peroxidase-Blocking Reagent included in the kit. The substrate system consists of 2 components: EnVision FLEX DAB + Chromogen (DM847), a concentrated diaminobenzidine (DAB) solution, and EnVision FLEX Substrate Buffer (DM843) containing hydrogen peroxide. Before use EnVision FLEX DAB + Chromogen must be diluted in EnVision FLEX Substrate Buffer. The substrate system produces a crisp brown end product at the site of the target antigen. Timely mixing of chromogen and buffer is automatically performed onboard Dako Omnis. Hematoxylin is recommended for counterstaining. The reagent provides a clear blue, nuclear staining.

The stained tissue sections are mounted with organic-solvent-based mounting medium.

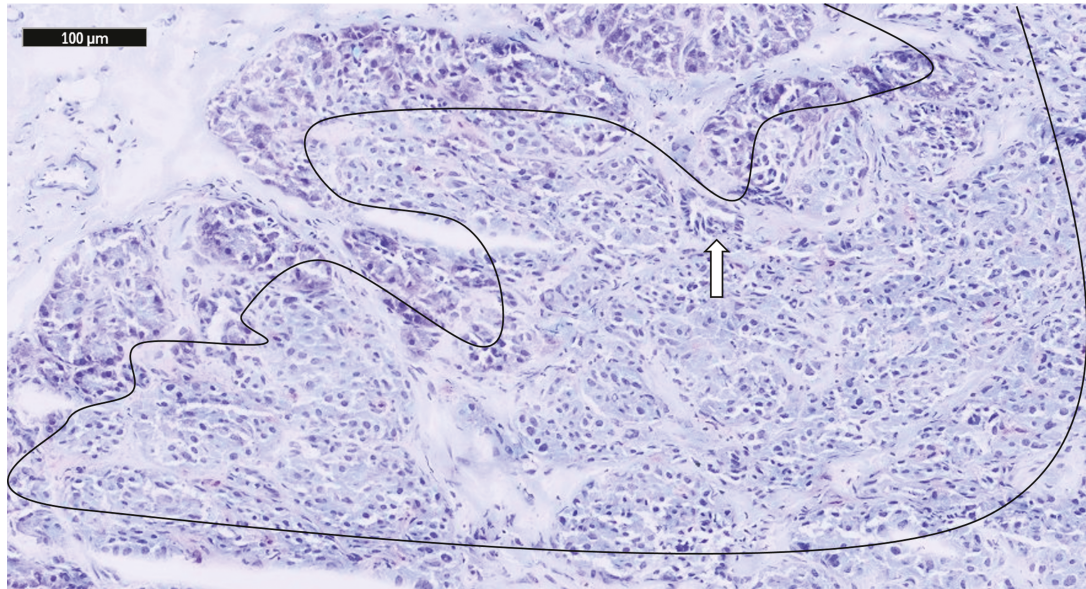
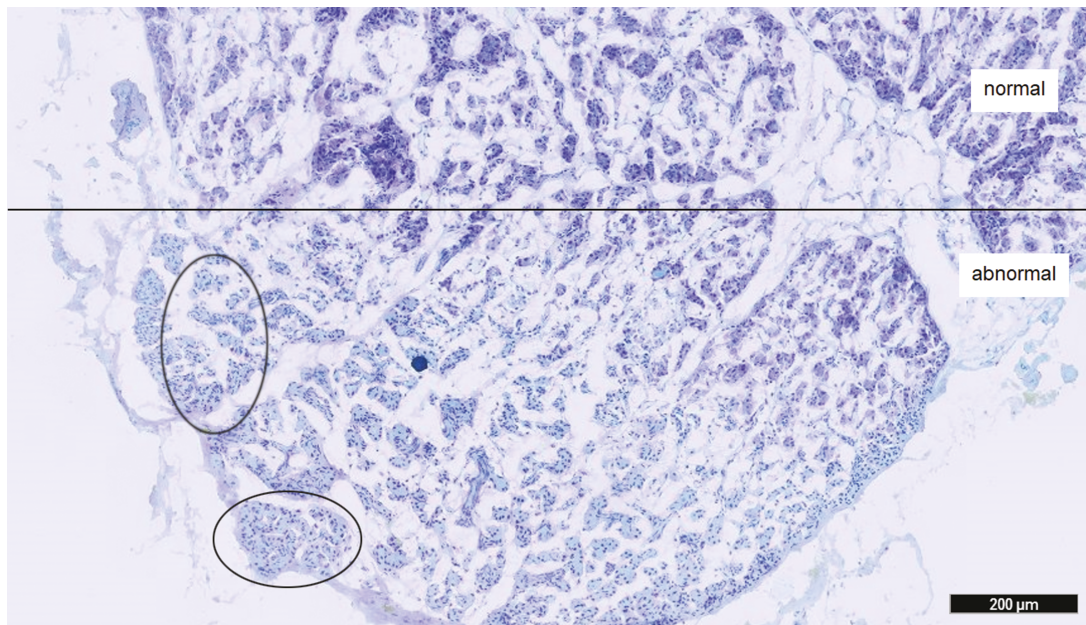
The histopathological examination of the 2 areas in the cranial edge of pancreatic neck and body that were described as possible areas of focal lesions on the PET-MRI showed small aggregates of ill-formed islet-like clusters with ductuloinsular complexes and some enlarged nuclei (Figs. 4 and 5). Fig. 6 shows regular parenchyma.

## Molecular Pathology

Genomic DNA was extracted from 2 native tissue samples from the resected tissue and from formalin-fixed, paraffin-embedded samples from various sites of the intraoperative biopsies. Exon 21 with flanking introns of the *ABCC8* gene was amplified by polymerase chain reaction, and bidirectional Sanger sequencing was performed using Big Dye Terminator Cycle Sequencing Kit and a 3500xl Genetic Analyzer (Applied Biosystems). Sequences were aligned to reference sequence ENST00000302539 using SeqPilot analysis software (JSI Medical Systems). LOH was estimated by comparing the area under the curve of electropherograms for the wild-type and mutant peaks in the forward and reverse sequencing

**Table 1.** List of antibodies for the histopathological examination

Antigen	Clone	Supplier	Dilution ratio	Platform	RRID
Chromogranin A	DAK-A3	Dako	1:1000	Dako Omnis	<a href="#">AB_2199013</a>
Synaptophysin	DAK-Synap	Dako	Ready to use	Dako Omnis	<a href="#">AB_2687942</a>
Insulin	2D11-H5	Leica	Ready to use	Dako Omnis	<a href="#">AB_563784</a>

**Figure 4.** Toluidine blue stain from frozen section number 6 (see Fig. 7). Focus-like structure consisting of an aggregate of ill-formed, islet-like cluster associated with a ductuloinsular complex (arrow). Some of the nuclei within the lesion are enlarged.**Figure 5.** Toluidine blue stain from frozen section number 10 (see Fig. 7). Upper half: parenchyma with regular architecture; lower half: parenchyma with some hyperplastic islets leading to a marked increase in size and structure.

directions using SeqPilot software. This analysis showed that the aforementioned 2 PET-MRI-identified areas had an LOH with the highest mutant allele fractions (MAF: 84% and 73%). The area in between showed only a slight LOH with a lower MAF, nearly normal heterozygosity.

Array-CGH was performed using a CytoScan HD microarray and the Chromosome Analysis Suite v4.3.0.71 (Thermo Fisher Scientific) for analysis to identify the genetic alteration underlying LOH. In DNA from 2 tissue specimens from distinct focal sites with high LOH (samples 7 and 11), we could

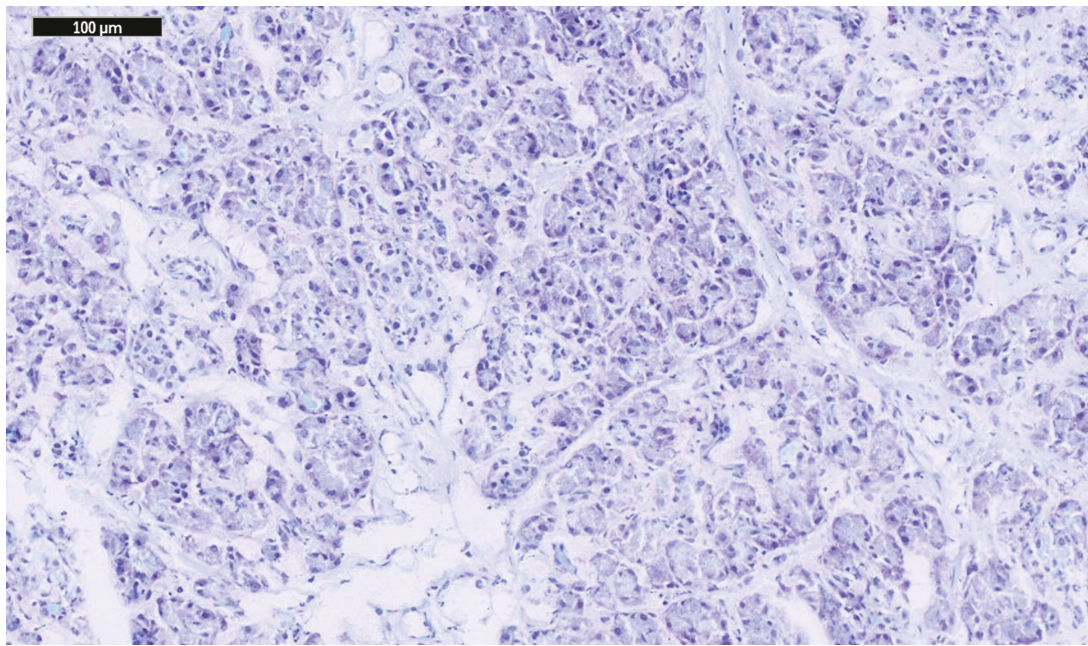


**Figure 6.** Toluidine blue stain from frozen section number 3 (see Fig. 7). Regular parenchyma with exocrine (acini and ducts) and endocrine (islets of Langerhans) tissue arranged in lobules separated by connective tissue.

demonstrate a segmental UPD, arr[GRCh37] 11p15.5p11.2 (1\_44800789) × 2 hmz [0.4 ~ 0.7], which was identical in both samples.

### Correlation of Magnetic Resonance Imaging, Surgery, Histopathology, and Genetics

Fig. 7 shows a map of the pancreas combining surgery biopsies, suspicious focal areas on MRI, histopathological results, and genetic findings within the specimens. The 2 distinct areas in the pancreas showed an obvious correlation of PET-MRI activity with histopathologic appearance and genetic LOH. These findings obviously corresponded to the region of functional alteration with uncontrolled insulin secretion, as indicated by the surgical success after removal only of these tissue regions. Both areas showed an identical UPD11p profile indicating that the large focal area with segmental expansion likely originated from a single precursor cell (Fig. 8).

### Discussion

In the case reported here, we were confronted with the question whether the patient had 1 large, complex focal lesion with 2 hot spots or a bifocal lesion. Few patients with separate bifocal lesions have been described before. Giurgea et al [10] and Rosenfeld et al [11] each reported 2 cases with bifocal lesions based on genetic examinations demonstrating differently sized regions of LOH in the foci from the same patient. Both authors postulated independent somatic events being causative for the separated focal pathologies. However, the probability of 2 independent second hits in the same individual should be very low: According to Glaser and colleagues [12] and Snider et al [13], the estimated risk of a second event causing focal CHI in a newborn who carries a paternally inherited recessive *ABCC8* or *KCNJ11* gene variant is around 1:250, which would give a probability of 1:62 500 for 2 independent events occurring in

an individual with a heterozygous paternally inherited pathogenic variant. Giurgea et al [10] in the same paper reported another case with a giant focal lesion involving a large part of the pancreas in which they found an identical somatic maternal 11p15 deletion in 2 independent lesion samples, suggesting a very early mutational event during pancreas embryogenesis. This is similar to our observation of a larger area of abnormal tissue with 2 major foci of increased metabolic activity, where we found an UPD11p of identical size in or nearby each of both hot spots (samples 11 and 7 in Fig. 7). Thereby, our observation further supports the notion that a somatic mutational event leading to LOH that arises during early development in a pancreatic precursor may give rise to a larger segmental area of affected tissue and atypical forms of focal CHI due to atypical mosaicism. In our case, another peculiarity was that the heterozygous *ABCC8* germline variant was not paternally inherited but a de novo event that has to be assumed to have arisen on the paternal allele. Taken together, we think that in our case we are dealing with 1 large, heterogeneous focal lesion with 2 distinct activity peaks and a bridge of pancreatic tissue between them demonstrating atypical histopathological architecture combined with a lower fraction of cells with LOH being capable of uncontrolled insulin secretion.

CHI can also be a feature of BWS, with severe and persistent CHI especially or even exclusively occurring in cases with mosaic paternal UPD11p as the underlying cause of the syndrome [14]. A few cases reported by Kalish et al [14] have been found to have a paternally inherited K-ATP variant in addition to their UPD11p, thus explaining the CHI on the basis of the established dual-hit mechanism. However, the majority of cases with severe and persistent CHI and BWS due to paternal UPD11p reported in this study were not associated with a K-ATP variant, suggesting that the paternal UPD11p per se can also initiate a K-ATP-independent mechanism for CHI. The authors proposed a combined mechanism of islet overgrowth due to the proliferative

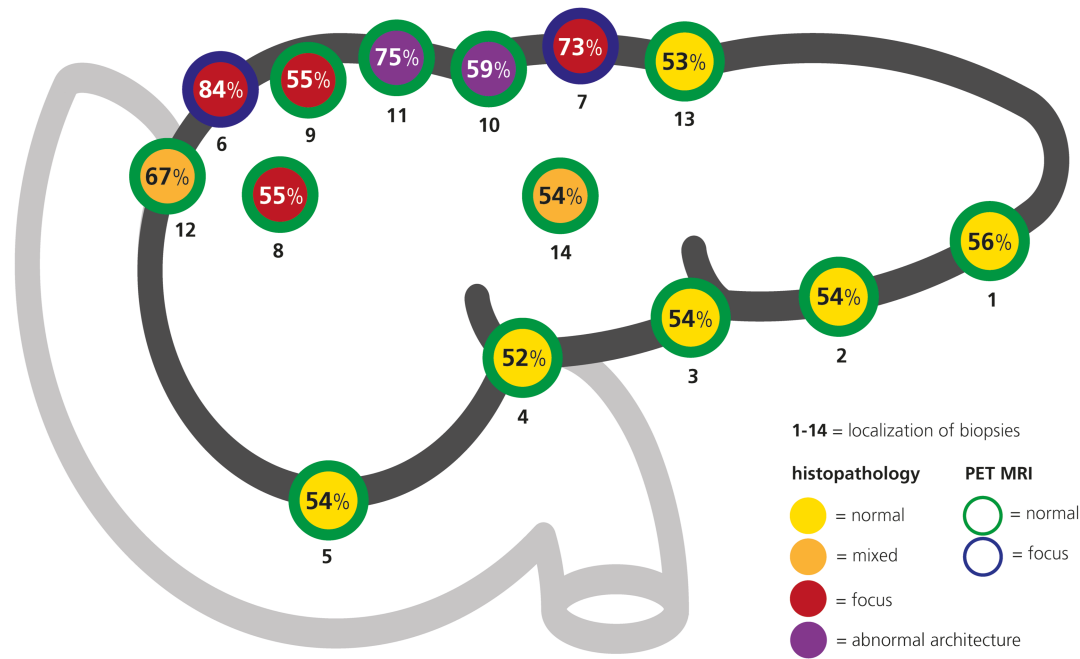


**Figure 7.** Anatomical localization of the specimen in the pancreas combined with the histopathological, genetic, and magnetic resonance imaging (MRI) findings. The circles symbolize the specimen taken during the operation. The inner color stands for histopathological findings and the border for the MRI findings. The number inside the circles stands for the mutant allele frequency.

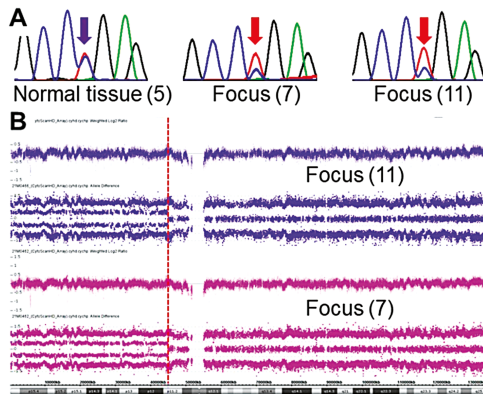


**Figure 8.** Microarray analysis. A, Sequence traces from a biopsy showing normal tissue (sample 5: 21M1620) and from 2 distinct focal lesions (sample 7: 21M0462 and sample 11: 21M0466). The mutant T allele peak is equal to the wild-type C allele in normal tissue (violet arrow), while the T allele (red trace color) is predominating in the specimens from focal lesions (orange arrows) due to loss of the wild-type allele in a significant proportion of cells. B, Chromosomal microarray analysis of the same focal lesions (sample 7: 21M0462 lower panel and sample 11: 21M0466 upper panel) show a mosaic pattern of segmental uniparental disomy (UPD) of the short arm of chromosome 11. The breakpoint of UPD in both samples is identical and localizes to chromosomal band 11p11.2 as indicated (vertical dashed red line).

effect of the paternal imprint pattern of the 11p15 region together with a lack of expression of the *KCNQ1* voltage-gated potassium channel that is expressed only from the maternal allele. *KCNQ1* itself is assumed to be involved in the regulation of potassium flux in pancreatic  $\beta$  cells [15]. Pancreatic histology in patients with CHI and BWS due to UPD11p shows a marked diffuse increase in the volume of endocrine tissue, often with a gradient in the degree of islet expansion across the entire pancreas [14].

In some patients in the case series reported by Kalish et al [14], the UPD11p was undetectable in blood. In our patient, the absence of prenatal overgrowth or other features of BWS, the focal appearance on imaging, the absence of UPD11p in peripheral leucocytes but detection of LOH in a very restricted area of the pancreas clearly argue against a more widespread mosaicism of UPD11p and a diagnosis of BWS.

A few other cases with a heterozygous pathogenic K-ATP variant plus mosaic UPD11p and atypical pancreatic histology with or without BWS features have been described (Table 2 [16-18]). Therefore, mosaic UPD11p combined with a pathogenic K-ATP variant may cause a large disease spectrum ranging from BWS with persistent CHI to nonsyndromic CHI cases with atypical pancreatic histology like the one described here. The expression within this spectrum likely depends on the timing of the mutational event leading to UPD11p during embryogenesis, with later events keeping a more restricted distribution and being less likely to produce conceivable systemic BWS features.

It is well known that focal lesions can present with a matrix capsule or without a clear separation from normal pancreatic tissue [19]. The onset of hypoglycemia in the first group was later than that of the second group, the surgery was easier to perform, and the outcome was better in view of normoglycemia. The focal regions of our child showed no clear margin, nevertheless, the resection was clinically successful. Focal lesions can be very heterogeneous; patients with the same genotype can present with different clinical presentations [20]. Another case report describes a focal lesion occupying nearly the whole pancreas that was seen only because of a second PET scan that was performed because of continuous hypoglycemia following resection of the first alleged focal area [21].

## Conclusions

A focal lesion in CHI can be heterogeneous, with distinct PET-MRI, histopathological, genetic, and functional

**Table 2.** Summary of clinical, genetic, localization, diagnostic, and histological findings of our and published cases

Reference	Clinical BWS	pUPD in peripheral leucocytes	pUPD pancreatic area	Variant in K <sub>ATP</sub> subunit	<sup>18</sup> F-DOPA-PET	Histology	
Our patient	No	No	Yes	<i>ABCC8</i> de novo	2 separate pancreatic foci in neck and body	2 adenomatous lesions and neighboring tissue showed abnormal architecture, no capsule, all other samples with suppressed pancreatic islets	
Giurgea et al; 2006	No	No	Yes	Paternal <i>ABCC8</i>	Not done	Compact adenomatous lesion in 95% of pancreas and 70%-80% of body, no hyperfunctional islets in inferior half of head and uncinata process of pancreas	
Tung et al; 2020	No	No	Yes	Paternal <i>ABCC8</i>	Multiple adenomatous hyperplasia	Atypical findings of coalescing nests and trabeculae of adenomatosis scattered with islets with isolated enlarged, hyperchromatic nuclei scattered throughout pancreas	
Calton et al; 2013	No	No	Yes	Paternal <i>ABCC8</i>	Focus in pancreatic head	Not reported	
Adachi et al; 2013	No	Yes	Not done	Paternal <i>ABCC8</i>	2 Pancreatic foci in head and body	Not done	
Kalish et al; 2016	Case 2	Yes	Yes	Yes	Paternal <i>ABCC8</i>	Increased uptake in tail	Throughout large areas of pancreas nuclei in ribbon or garland-like pattern, gradient in degree of islet expansion across entire pancreas
	Case 3	Yes	No	Yes	Paternal <i>ABCC8</i>	Not reported	
	Case 7	No	Yes	Yes	Paternal <i>KCNJ11</i>	Not reported	
	Case 9	Yes	Yes	Yes	Paternal <i>KCNJ11</i>	Not reported	
Kocaay et al; 2016	Yes	Yes	Yes	Paternal <i>KCNJ11</i>	Not done	Diffuse	

Abbreviations: <sup>18</sup>F-DOPA, fluorine-18-L-dihydroxyphenylalanine; BWS, Beckwith Wiedemann syndrome; K-ATP, adenosine 5'-triphosphate-sensitive potassium; PET, positron emission tomography; pUPD, paternal uniparental disomy.

appearances. The number and timing of secondary genetic events leading to LOH of 11p seem to be major determinants for this heterogeneity. A focal CHI with complex morphology can be clinically cured by precise tissue-saving surgery selectively resecting only the most active areas.

## Acknowledgments

The authors are indebted to Dr Matthew Tytherleigh, consultant general surgeon, for his invaluable contribution in reviewing the manuscript and checking it with regard to English language and consistency. All authors attest that they meet the current ICMJE criteria for authorship. Consent to publish this case report was not obtained because this report does not contain any personal information that could lead to the identification of the patient.

## Financial Support

The authors received no financial support for the research, authorship, and/or publication of this article.

## Disclosures

The authors have nothing to disclose.

## Data Availability

Some of the data sets generated during and/or analyzed during the present study are not publicly available but are available from the corresponding author on reasonable request.

## References

1. Arnoux JB, de Lonlay P, Ribeiro MJ, et al. Congenital hyperinsulinism. *Early Hum Dev.* 2010;86(5):287-294.
2. Banerjee I, Salomon-Estebanez M, Shah P, Nicholson J, Cosgrove KE, Dunne MJ. Therapies and outcomes of congenital hyperinsulinism-induced hypoglycaemia. *Diabet Med.* 2019;36(1):9-21.
3. Demirbilek H, Hussain K. Congenital hyperinsulinism. Diagnosis and treatment update. *J Clin Res Pediatr Endocrinol.* 2017;9(Suppl 2):69-87.
4. Rosenfeld E, Ganguly A, De León DD. Congenital hyperinsulinism disorders. Genetic and clinical characteristics. *Am J Med Genet C Semin Med Genet.* 2019;181(4):682-692.
5. Sempoux C, Capito C, Bellanné-Chantelot C, et al. Morphological mosaicism of the pancreatic islets: a novel anatomopathological form of persistent hyperinsulinemic hypoglycemia of infancy. *J Clin Endocrinol Metab.* 2011;96(12):3785-3793.
6. Barthlen W, Varol E, Empting S, et al. Surgery in focal congenital hyperinsulinism (CHI)—the “Hyperinsulinism Germany International” experience in 30 children. *Pediatr Endocrinol Rev.* 2016;14(2):129-137.

7. Adzick NS, De Leon DD, States LJ, *et al.* Surgical treatment of congenital hyperinsulinism: Results from 500 pancreatectomies in neonates and children. *J Pediatr Surg.* 2019;54(1):27-32.
8. Tung JYL, Lai SHY, Au SLK, *et al.* Coexistence of paternally-inherited *ABCC8* mutation and mosaic paternal uniparental disomy 11p hyperinsulinism. *Int J Pediatr Endocrinol.* 2020;2020:13.
9. Rahier J, Guiot Y, Sempoux C. Morphologic analysis of focal and diffuse forms of congenital hyperinsulinism. *Semin Pediatr Surg.* 2011;20(1):3-12.
10. Giurgea I, Sempoux C, Bellanné-Chantelot C, *et al.* The Knudson's two-hit model and timing of somatic mutation may account for the phenotypic diversity of focal congenital hyperinsulinism. *J Clin Endocrinol Metab.* 2006;91(10):4118-4123.
11. Rosenfeld E, Mitteer L, Boodhansingh K, *et al.* Case report: two distinct focal congenital hyperinsulinism lesions resulting from separate genetic events. *Front Pediatr.* 2021;9:699129.
12. Glaser B, Blech I, Krakivinsky Y, *et al.* *ABCC8* mutation allele frequency in the Ashkenazi Jewish population and risk of focal hyperinsulinemic hypoglycemia. *Genet Med.* 2011;13(10):891-894.
13. Snider KE, Becker S, Boyajian L, *et al.* Genotype and phenotype correlations in 417 children with congenital hyperinsulinism. *J Clin Endocrinol Metab.* 2013;98(2):E355-E363.
14. Kalish JM, Boodhansingh KE, Bhatti TR, *et al.* Congenital hyperinsulinism in children with paternal 11p uniparental isodisomy and Beckwith-Wiedemann syndrome. *J Med Genet.* 2016;53(1):53-61.
15. Lubberding AF, Zhang J, Lundh M, *et al.* Age-dependent transition from islet insulin hypersecretion to hyposecretion in mice with the long QT-syndrome loss-of-function mutation *Kcnq1-A340V*. *Sci Rep.* 2021;11(1):12253.
16. Calton EA, Temple IK, Mackay DJ, *et al.* Hepatoblastoma in a child with a paternally-inherited *ABCC8* mutation and mosaic paternal uniparental disomy 11p causing focal congenital hyperinsulinism. *Eur J Med Genet.* 2013;56(2):114-117.
17. Adachi H, Takahashi I, Higashimoto K, *et al.* Congenital hyperinsulinism in an infant with paternal uniparental disomy on chromosome 11p15: few clinical features suggestive of Beckwith-Wiedemann syndrome. *Endocr J.* 2013;60(4):403-408.
18. Kocaay P, Şiklar Z, Ellard S, *et al.* Coexistence of mosaic uniparental isodisomy and a *KCNJ11* mutation presenting as diffuse congenital hyperinsulinism and hemihypertrophy. *Horm Res Paediatr.* 2016;85(6):421-425.
19. Craigie RJ, Salomon-Estebanez M, Yau D, *et al.* Clinical Diversity in Focal Congenital Hyperinsulinism in Infancy Correlates with Histological Heterogeneity of Islet Cell Lesions. *Front Endocrinol (Lausanne).* 2018;9:619.
20. Ismail D, Smith VV, de Lonlay P, *et al.* Familial focal congenital hyperinsulinism. *J Clin Endocrinol Metab.* 2011;96(1):24-28.
21. Ismail D, Kapoor RR, Smith VV, *et al.* The heterogeneity of focal forms of congenital hyperinsulinism. *J Clin Endocrinol Metab.* 2012;97(1):E94-E99.